THE JOURNAL OF BIOLOGICAL CHEMISTRY VOL. 284, NO. 11, pp. 6982–6987, March 13, 2009

Localization and Structure of the Ankyrin-binding Site on β_2-Spectrin*

Received for publication, December 9, 2008 Published, JBC Papers in Press, December 20, 2008, DOI 10.1074/jbc.M809245200

Lydia Davis[‡], Khadar Abdi[‡], Mischa Machius[§], Chad Brautigam[§], Diana R. Tomchick[§], Vann Bennett[‡], and Peter Michaely[¶1]

From the [‡]Department of Cell Biology and Howard Hughes Medical Institute, Duke University Medical Center, Durham, North Carolina 27710 and the Departments of [§]Biochemistry and [¶]Cell Biology, University of Texas Southwestern Medical Center, Dallas, Texas 75390-9039

Spectrins are tetrameric actin-cross-linking proteins that form an elastic network, termed the membrane skeleton, on the cytoplasmic surface of cellular membranes. At the plasma membrane, the membrane skeleton provides essential support, preventing loss of membrane material to environmental shear stresses. The skeleton also controls the location, abundance, and activity of membrane proteins that are critical to cell and tissue function. The ability of the skeleton to modulate membrane stability and function requires adaptor proteins that bind the skeleton to membranes. The principal adaptors are the ankyrin proteins, which bind to the β-subunit of spectrin and to the cytoplasmic domains of numerous integral membrane proteins. Here, we present the crystal structure of the ankyrin-binding domain of human β_2-spectrin at 1.95 Å resolution together with mutagenesis data identifying the binding surface for ankyrins on β_2-spectrin.

Spectrin is the principal component of a membrane-associated cytoskeletal network termed the membrane skeleton. The membrane skeleton was first identified in human erythrocytes, where it lines the cytoplasmic surface of the plasma membrane and provides the viscoelastic support necessary for erythrocytes to withstand the shear stresses experienced during blood circulation (1). Subsequently, the membrane skeleton was characterized on the plasma membranes of most cells, where the skeleton not only supports the plasma membrane but also promotes the polarized distribution of cell adhesion molecules and ion transport proteins (2–4). In addition, the membrane skeleton is present on the cytoplasmic surface of intracellular membrane compartments; however, the function of the skeleton on most intracellular compartments is not clear.

The membrane skeleton is composed of spectrins, actin filaments, and a collection of accessory proteins. Spectrins are tetrameric proteins composed of two α-spectrins and two β-spectrins that together form ~220-nm-long elastic filaments (2). In mammals, spectrin proteins are expressed from two α-spectrin genes (α_1 and α_2) and five β-spectrin genes (β_1–β_5). The most abundant protein motifs of both α- and β-spectrins are spectrin repeats, which are present in 21 copies in α-spectrins and 16 copies in most β-spectrins (see Fig. 1). Spectrin repeats are ~106-amino acid motifs that form three-helix coiled-coils. The principal function of the spectrin repeat is to confer elasticity to spectrin (5, 6); however, repeat 15 of most β-spectrins also has the ability to bind to the ankyrin family of accessory proteins (7). Ankyrins are adaptor proteins that bind the membrane skeleton to membranes through their ability to associate with the cytoplasmic domains of at least 12 distinct families of integral membrane proteins (3). Mammals have three ankyrin genes (*Ank1*, *Ank2*, and *Ank3*), each of which produces a family of proteins (ankyrin-R, -B, and -G, respectively) through alternative splicing. Defects in specific ankyrins or spectrins disrupt membrane linkages that are required for normal cell function in specific tissues and cause a variety of hereditary diseases, including hemolytic anemia, cardiac arrhythmia, premature aging, deafness, and ataxia (4, 8).

Despite the importance of the spectrin-ankyrin association, a structural basis for the interaction has not been established. Structure prediction algorithms suggest that repeat 15 of β-spectrins adopts a three-helix bundle conformation similar to other spectrin repeats; however, sequence comparisons have suggested that repeat 15 has unique features that may confer ankyrin-binding activity (7). Here, we provide a 1.95 Å resolution crystal structure of spectrin repeats 14–16 of human β_2-spectrin. We also provide mutational data that identify the ankyrin-binding surface on repeat 15 of β_2-spectrin.

EXPERIMENTAL PROCEDURES

Protein Expression and Purification—cDNA encoding spectrin repeats 14–16 of human β_2-spectrin was synthesized by PCR and ligated into the pET15b expression vector (Novagen). The resulting plasmid was then transformed into the *Escherichia coli* strain BL21(DE3). Expression of B14–16 protein was induced by 1 mM isopropyl β-D-thiogalactopyranoside, and expressed B14–16 was purified by sequential column chroma-

* This work was supported, in whole or in part, by National Institutes of Health Grant HL085218 from NHLBI. The structure shown in this study was derived from work performed on beamline 19-ID at the Argonne National Laboratory Structural Biology Center at the Advanced Photon Source, which is operated by UChicago Argonne, LLC, for the United States Department of Energy, Office of Biological and Environmental Research, under Contract DE-AC02-06CH11357. The costs of publication of this article were defrayed in part by the payment of page charges. This article must therefore be hereby marked "*advertisement*" in accordance with 18 U.S.C. Section 1734 solely to indicate this fact.

The atomic coordinates and structure factors (code 3EDV) have been deposited in the Protein Data Bank, Research Collaboratory for Structural Bioinformatics, Rutgers University, New Brunswick, NJ (http://www.rcsb.org/).

[1] To whom correspondence should be addressed: Dept. of Cell Biology, University of Texas Southwestern Medical Center, 5323 Harry Hines Blvd., Dallas, TX 75390-9039. Tel.: 214-648-3238; Fax: 214-648-8694; E-mail: Peter.Michaely@utsouthwestern.edu.

tography using nickel-nitrilotriacetic acid-agarose, Q-Sepharose, and Superose12. The selenomethionine (SeMet)[2] variant of B14–16 was expressed in the methionine auxotrophic *E. coli* strain B834(DE3) and grown in minimal medium supplemented with natural amino acids and SeMet. Expression and purification were unchanged.

Crystallization and X-ray Diffraction Data Collection—Crystals of B14–16 were grown using the hanging-drop vapor diffusion method from drops containing 1 μl of protein (25 mg/ml) and 1 μl of reservoir solution (14% polyethylene glycol 4000, 100 mM Tris (pH 8.5), and 300 mM $MgCl_2$) and equilibrated over 200 μl of reservoir solution. Disphenoidal crystals appeared after 3–4 days at 4 °C and grew to their maximal extent by 2 weeks. Crystals were small (0.1-mm maximal length) and thin (0.02-mm thickness). SeMet protein crystallized in an identical fashion. Cryoprotection was performed by increasing the glycerol content in reservoir solution up to 30% in 5% steps over the course of 30 min at 4 °C. Crystals were flash-frozen using liquid propane. Crystals exhibited the symmetry of space group $P2_12_12_1$ with unit cell parameters of a = 51.3, b = 56.1, and c = 261.6 Å and contained two molecules of B14–16 per asymmetric unit. Native crystals diffracted isotropically to a d_{min} of 1.95 Å and SeMet crystals to a d_{min} of 2.4 Å when exposed to synchrotron radiation. Data were indexed, integrated, and scaled using the HKL3000 program package (9). Data collection statistics are provided in Table 1.

Phase Determination and Structure Refinement—Phases were obtained from a single-wavelength anomalous dispersion experiment using a SeMet-B14–16 crystal with data to a resolution of 2.4 Å. Eighteen selenium sites were located using the program SHELXD (10); this represented five single-occupancy sites and two double-conformation sites per B14–16 monomer. Phases were refined with the program MLPHARE (11), resulting in an overall figure of merit of 0.18 for data between 50.0 and 2.4 Å. Phases were further improved by density modification and 2-fold non-crystallographic averaging with the program DM (12), resulting in a figure of merit of 0.67. An initial model containing ~95% of all residues was automatically generated by alternating cycles of the program ARP/wARP (13).

Additional residues were manually modeled in the programs O (14) and Coot (15). Refinement was performed with native data to a resolution of 1.95 Å using the programs PHENIX and REFMAC (16) with a random 5.1% of all data set aside for an R_{free} calculation. The current model contains two B14–16 monomers (molecule A with residues 1697–2015 and molecule B with residues 1697–2014), 561 waters, one molecule of Tris, four molecules of glycerol, and one magnesium ion. Two and three residues of vector sequence were also modeled at the N terminus of molecules A and B, respectively, of B14–16. Sixteen residues were modeled in alternate conformations. The R_{work} is 0.198, and the R_{free} is 0.255. A Ramachandran plot generated with MolProbity (17) indicated that 99.7% of all protein residues are in the most favored regions with the remaining 0.3% in additionally allowed regions. Phasing and model refinement statistics are provided in Table 1.

[2] The abbreviation used is: SeMet, selenomethionine.

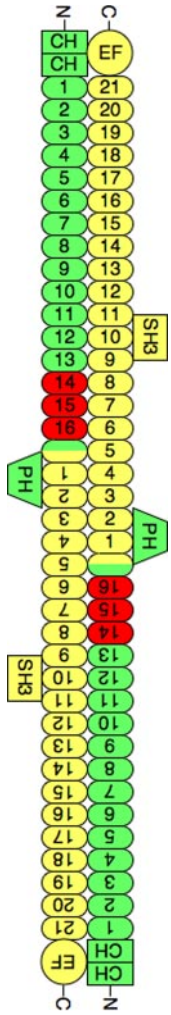

FIGURE 1. **B14–16 region of the spectrin tetramer.** The diagram shows the arrangement of α_2- and β_2-spectrins in the spectrin tetramer along with the domain organization of each subunit. α-Spectrin is colored *yellow*, and β-spectrin is colored *green*. Spectrin repeats are indicated by number. Shown in *red* are the spectrin repeats of β-spectrin that were crystallized. The Src homology 3 (*SH3*) domain in α_2-spectrin is an insert in spectrin repeat 10. *EF* refers to the EF-hand domains at the C terminus of α_2-spectrin, which bind to calcium. In β-spectrin, the CH motifs bind to actin, whereas the pleckstrin homology (*PH*) domain binds to lipids. The end-to-end association of α- and β-spectrin is mediated by partial spectrin repeats that form a three-helix bundle consisting of one helix from α-spectrin and two helices from β-spectrin.

Yeast Two-hybrid Analysis—Nucleotides 4689–6279 of the human β_2-spectrin cDNA were fused to the cDNA of the Gal4 activation domain in the pACT2 vector. Mutations in the repeat 15 region of β_2-spectrin were introduced using QuikChange (Stratagene). Nucleotides 2584–4329 of the human ankyrin-B cDNA or nucleotides 2620–4428 of the human ankyrin-G cDNA (encoding the spectrin-binding domains of the respective ankyrins) were fused to the cDNA of the Gal4 DNA-binding domain in the pAS2-1 vector. Yeast were cotransformed with recombinant pACT2 and pAS2-1 vectors and grown for 6 days on agar plates either lacking leucine and tryptophan or lacking adenine, histidine, leucine, and tryptophan. All yeast strains grew on agar lacking leucine and tryptophan. Growth on agar lacking adenine, histidine, leucine, and tryptophan was scored as ++ for strong growth, + for moderate growth, and − for no growth.

TABLE 1

Data collection, phasing, and refinement statistics for the spectrin B14–16 structure

Data for the outermost shell are given in parentheses. r.m.s.d., root mean square deviation.

Data collection		
Crystal	Native	SeMet[a]
Energy (eV)	12,661.7	12,660
Resolution range (Å)	43.60–1.95 (1.97–1.95)	47.9–2.40 (2.42–2.40)
Unique reflections	55,069 (1,174)	29,026 (438)
Multiplicity	4.2 (3.4)	6.0 (2.2)
Data completeness (%)	97.3 (86.1)	93.4 (57.5)
R_{merge} (%)[b]	4.6 (68.2)	7.6 (25.5)
$I/\sigma(I)$	29.4 (1.97)	33.8 (3.47)
Wilson B-value (Å^2)	30.2	42.7
Phase determination		
Anomalous scatter	Selenium, 18 out of 18 possible sites	
Figure of merit (30-2.40 Å)	0.18 (0.67 after density modification)	
Refinement statistics		
Resolution range (Å)	28.6–1.95 (1.98–1.95)	
No. of reflections (R_{work}/R_{free})	52,170/2788 (2241/111)	
Data completeness (%)	97.2 (85.0)	
Atoms (non-H protein/solvent/other)	5479/561/33	
R_{work} (%)	19.2 (24.0)	
R_{free} (%)	25.0 (32.9)	
r.m.s.d. bond length (Å)	0.008	
r.m.s.d. bond angle	0.845°	
Mean B-value (Å; protein/solvent/other)	39.6/44.8/64.4	
Ramachandran plot (%; favored/additional/disallowed)[c]	99.7/0.3/0.0	
Maximum likelihood coordinate error	0.31	
Missing residues	Chain A, none; chain B, Leu^{2015}	
Alternate conformations	Chain A, 8; chain B, 8	

[a] Bijvoet pairs were kept separate for data processing.

[b] $R_{merge} = 100\,\Sigma_h\Sigma_i|I_{h,i} - \langle I_h\rangle|/\Sigma_h\Sigma_i I_{h,i}$, where the outer sum ($h$) is over the unique reflections, and the inner sum (i) is over the set of independent observations of each unique reflection.

[c] This was as defined by the validation suite MolProbity (17).

Figure Preparation—Structure figures were rendered using the MegaPOV extension of POV-Ray with primitive files produced using Coot (Fig. 2) (15), PyMOL (Figs. 3 and 6*C*) (DeLano Scientific LLC), or Swiss-PdbViewer (Figs. 4 and 5) (18).

RESULTS

Structure Determination and Description—A recombinant protein containing spectrin repeats 14–16 (Fig. 1) of human β_2-spectrin (B14–16) was purified from *E. coli* and crystallized. The crystal structure was solved by the single-wavelength anomalous dispersion method using SeMet-substituted B14–16 protein crystals. The Se-Met crystals diffracted to 2.4 Å, and single-wavelength anomalous dispersion phasing of these data generated an electron density map that was used to produce an initial model. Native crystals diffracted to 1.95 Å, and phases were extended to this limit using the 2.4 Å structure as an initial model. The asymmetric unit contained two molecules of B14–16, 561 waters, one molecule of Tris, four molecules of glycerol and one magnesium ion. The final model had an R_{work} of 19.8% and an R_{free} of 25.5% at 1.95 Å resolution. Statistics for the data collection and representative electron density are shown in Table 1 and Fig. 2.

The structure of B14–16 consists of three spectrin repeats connected by two linkers (Fig. 3). Each spectrin repeat forms an α-helical bundle consisting of three helices (A, B, and C) and two loops (AB and BC). For the purposes of this study, the helices and loops have been designated by repeat number and structural element (*e.g.* helix-14A refers to the A-helix of repeat 14, loop-15BC refers to the BC-loop of repeat 15). All helices show typical helical hydrogen bond networks with the exception of helix-15B and helix-16B. These helices are kinked near their midpoints and have ordered waters that form hydrogen bonds with backbone amide and carbonyl oxygens at the kink. The linkers between repeats are helical and are contiguous with the C-helix of the preceding repeats and the A-helix of the suc-

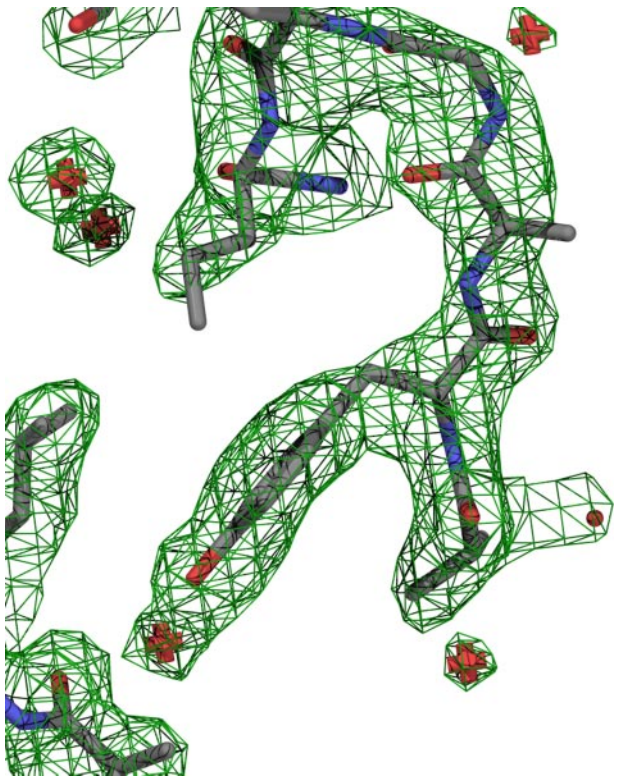

FIGURE 2. **Representative electron density.** Shown is the representative electron density near Tyr^{1874} with the final model shown as *sticks*. Carbons are colored *gray*; nitrogens, *blue*; and oxygens, *red*. Waters are shown as *red pluses*. Electron density at 1σ is shown as a *green wire network*.

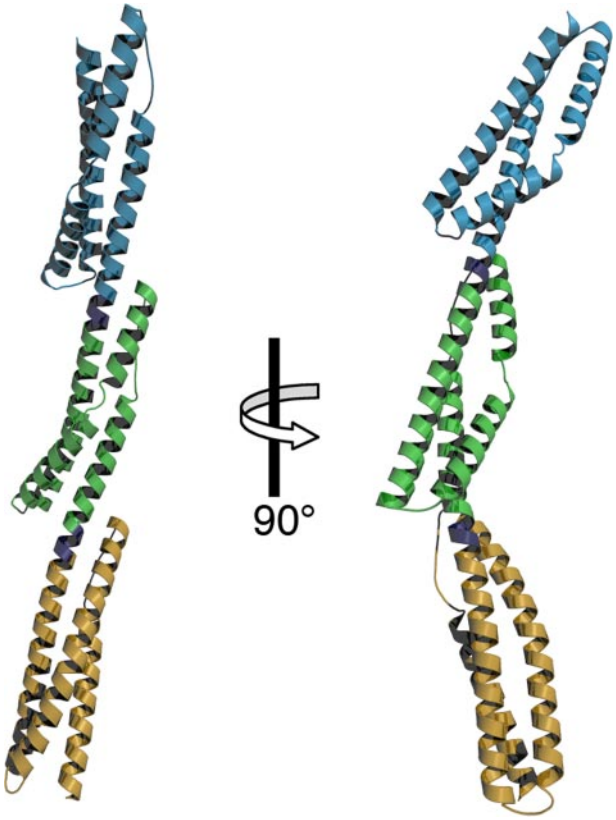

FIGURE 3. **Crystal structure of B14–16.** Shown are orthogonal ribbon representations of the crystal structure of B14–16. Repeat 14 is colored *tan*; repeat 15, *green*; and repeat 16, *blue*. The linkers connecting repeats are colored *purple*.

ceeding repeats. The overall structure of B14–16 is elongated with axial dimensions of 156 × 45 Å.

Each helix has a heptad pattern of hydrophobic residues that is typical of α-helical coiled-coils (19). These hydrophobic residues form an interlocking network of van der Waals contacts at the core of each spectrin repeat. As part of this heptad pattern, spectrin repeats commonly have tryptophan at position 17 in the A-helix and leucine near the end of the C-helix (20). Repeats 14 and 16 have both conserved residues; however, repeat 15 has an arginine (Arg^{1820}) in place of the tryptophan at position 17. Arg^{1820} is not part of the hydrophobic core: instead, the side chain of Leu^{1856} of helix-15B lies in the space normally occupied by tryptophans at position 17 (Fig. 4). Leu^{1856} can occupy space in the core because the B-helix of repeat 15 is rotated ~45° relative to the B-helices of repeats 14 and 16. This rotation points the side chain of Leu^{1856} toward the core, unlike the corresponding residues in repeats 14 and 16, which are oriented along the edge of the core.

Between individual repeats are helical linkers that join the C-helices of preceding repeats with the A-helices of succeeding repeats into one long continuous helix. In the B14–16 structure, van der Waals contacts between repeats dictate the orientation of neighboring repeats about the helical linker. At the N-terminal end of the interface, residues in the linker contact residues in the BC-loop of the succeeding repeat, whereas at the C-terminal end of the interface, residues of the AB-loop of the preceding repeat contact residues from two turns of the A-helix

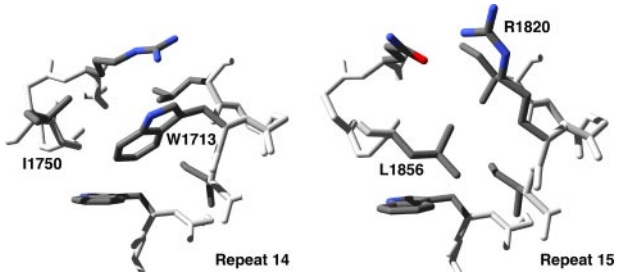

FIGURE 4. **Repeat 15 has a unique hydrophobic core near Arg^{1820}.** Most spectrin repeats have a characteristic tryptophan at position 17 of the A-helix that forms part of the hydrophobic core as exemplified in repeat 14 by Trp^{1713} (*A*). In repeat 15, Arg^{1820} resides at position 17, and the hydrophobic core is centered on Leu^{1856} from helix-15B (*B*).

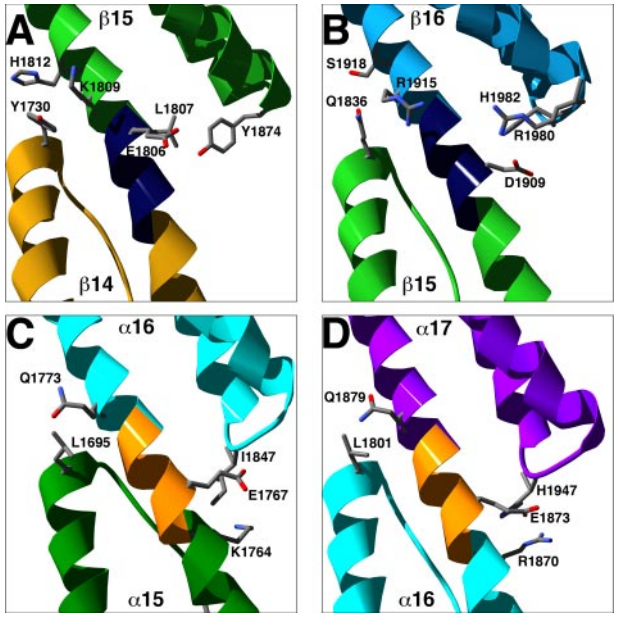

FIGURE 5. **Inter-repeat contacts control orientation between repeats.** Shown are ribbon representations of the inter-repeat junctions between repeats 14/15 (*A*) and repeats 15/16 (*B*) of β_2-spectrin and the inter-repeat junctions between repeats 15/16 (*C*) and repeats 16/17 (*D*) of α_2-spectrin. Linkers are colored *dark blue* in β_2-spectrin and *orange* in α_2-spectrin. Terminal residues of the inter-repeat contacts are labeled and shown as *sticks*.

of the succeeding repeat (Fig. 5, *A* and *B*). Comparison of the inter-repeat contacts of B14–16 with the previously described contacts between repeats 15–17 of α_2-spectrin (21) suggests that differences in the inter-repeat contacts contribute to the curvature differences in the two structures. In contrast to the B14–16 inter-repeat contacts, the interfaces in the α_2-spectrin structure have less extensive contacts between the AB-loop and the A-helix and have additional contacts between the C-helix and the BC-loop (Fig. 5, *C* and *D*). These differences specify a different orientation between repeats in the α_2- and β_2-spectrin structures. In repeats 15–17 of α_2-spectrin, the inter-repeat contacts specify a nearly straight concatomer of repeats, whereas in repeats 14–16 of β_2-spectrin, the contacts specify a substantial bend (Fig. 3). Consistent with the observed differences in curvature, electron micrographs of purified spectrin tetramers frequently show greater curvature near their midpoints (22, 23), where repeats 14–16 of β-spectrins reside (Fig. 1).

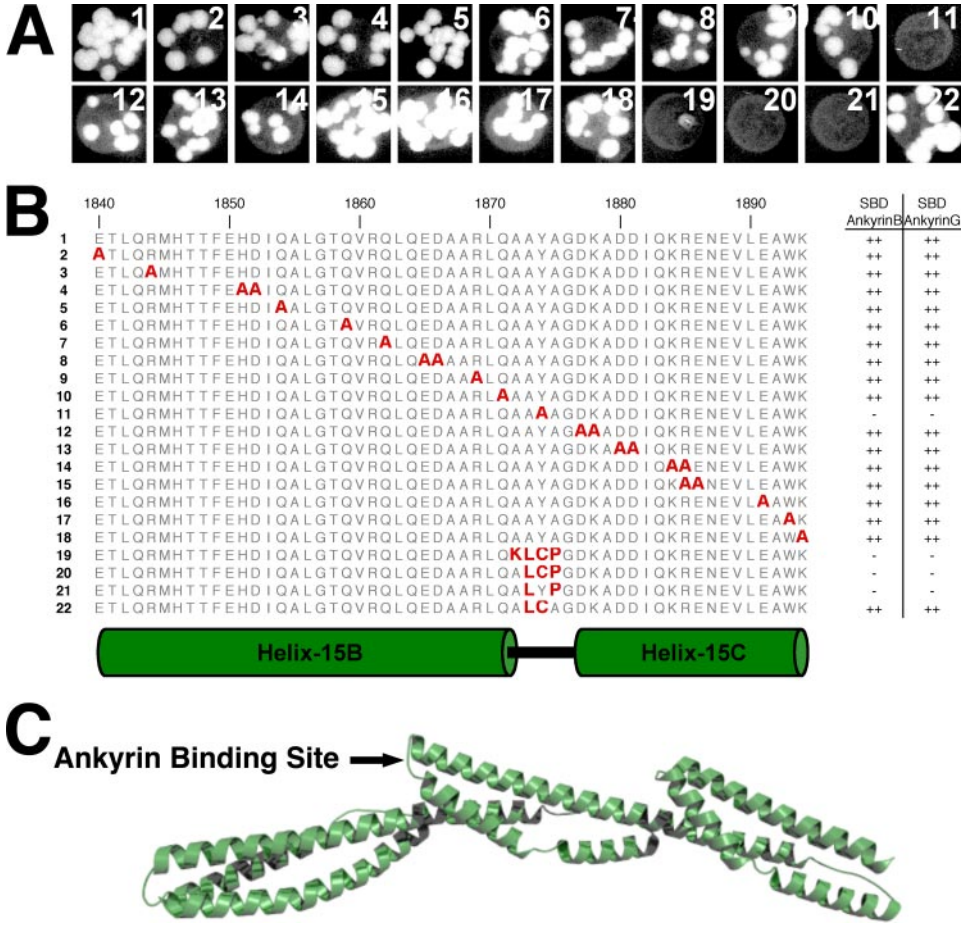

FIGURE 6. **Tyr[1874] of loop-15BC is required for ankyrin binding to repeats 14–16 of β_2-spectrin.** β_2-Spectrin variants with alanine mutations at 23 surface-exposed residues from helix-15B, loop-15BC, and helix-15C were screened for the ability to bind to the spectrin-binding domain (*SBD*) of ankyrin-B and ankyrin-G by yeast two-hybrid analyses. Shown in *A* is growth of yeast strains expressing the indicated spectrin variants fused to the Gal4 activation domain and the ankyrin-B spectrin-binding domain fused to the Gal4 DNA-binding domain on plates deficient for adenosine, histidine, leucine, and tryptophan. Similar results were observed in yeast strains expressing the spectrin variants together with the ankyrin-G spectrin-binding domain (yeast growth not shown). The location of individual mutations relative to secondary structure elements is shown in *B* alongside relative growth ability as indicated by ++ for strong growth and − for no growth. The location of the proposed ankyrin-binding site is indicated on the B14–16 structure in *C*.

Ankyrin-binding Site—Kennedy *et al.* (7) used deletion analysis to localize the ankyrin-binding site to repeat 15 and suggested, based upon sequence comparisons, that helix-15B played a role in ankyrin binding. We used yeast two-hybrid analyses to test whether exposed residues of helix-15B are required for ankyrin binding. Alanine mutations were made at 11 surface-exposed residues of helix-15B and tested for their effect on ankyrin binding using the spectrin-binding domains of ankyrin-B and ankyrin-G. None of the 11 mutations prevented the yeast two-hybrid reaction between repeats 13–16 of β_2-spectrin and the spectrin-binding domain of either ankyrin-B or ankyrin-G (Fig. 6), suggesting that helix-15B does not play a significant role in ankyrin binding.

We next examined helix-15C because the point mutation A1884V in helix-15C of β_1-spectrin is associated with hereditary spherocytosis (24). Ten surface-exposed residues of helix-15C were mutated to alanine and tested for ankyrin-binding ability using yeast two-hybrid analyses. As with mutations on helix-15B, none of the mutations in helix-15C prevented ankyrin binding (Fig. 6). Ala[1884] of β_1-spectrin corresponds to Ala[1892] of β_2-spectrin, which resides in a hydrophobic pocket formed by Phe[1818], Ile[1821], and Gln[1822]. This pocket does not have sufficient space to accommodate a valine, and the A1884V mutation in β_1-spectrin may disrupt the structure of repeat 15.

Finally, we tested whether loop-15BC plays a role in ankyrin binding. Loop-15BC consists of the sequence AAYA[1875], and in contrast to the mutations in the B- and C-helices, mutation of the surface-exposed Tyr[1874] to alanine abrogated the yeast two-hybrid interaction with ankyrin (Fig. 6). The AAYA sequence is well conserved between different β-spectrins with the exception of β_5-spectrin. β_5-Spectrin does not bind to ankyrins (25), and replacement of the BC-loop sequence of β_2-spectrin (AAYA[1875]) with the corresponding residues of spectrin repeat 15 of β_5-spectrin (KLCP[1907]) also abrogated ankyrin binding (Fig. 6). Together, these observations show that ankyrins bind to loop-15BC of β-spectrins.

DISCUSSION

The spectrin-ankyrin linkage provides the principal mechanism by which the mechanical properties of spectrin are coupled to membranes. Ankyrin binds to spectrin repeat 15 of β-spectrins, and sequence comparisons suggested that repeat 15 has unique features that confer ankyrin binding (7). The crystal structure of B14–16 shows that the sequence differences in repeat 15 produce only minor structural differences (Fig. 3). The most pronounced structural difference is a small rotation in helix-15B, which is associated with a unique feature in the hydrophobic core in which Leu[1856] of the B-helix fills space normally occupied in other spectrin repeats by tryptophans from the A-helix (Fig. 4). Consequences of the rotation in helix-15B partially explain the reported sequence differences of repeat 15 (7) but do not explain why ankyrin binds specifically to repeat 15 because alanine mutagenesis experiments suggest that helix-15B does not play a major role in ankyrin binding (Fig. 6).

Further mutagenesis experiments also failed to detect a role for helix-15C; however, substitution of alanine at Tyr[1874] in loop-15BC did impair ankyrin binding (Fig. 6). Loop-15BC consists of the sequence AAYA[1875], which forms a relatively flat, uncharged surface (Fig. 2) that has the potential to form van der

Waals and hydrogen bond contacts. These types of contacts are strengthened by moderate ionic strength, and the ankyrin-dependent interaction of spectrin with membranes is most stable at moderate ionic strength (23, 26), consistent with a role for loop-15BC in ankyrin binding. Interestingly, the AAYA^{1875} → ALCA variant also supported ankyrin binding, and modeling of the ALCA variant suggests that the ALCA sequence forms a flat uncharged surface similar to the AAYA sequence (data not shown). By contrast, the A1875P mutation likely disrupts the structure of loop-15BC because Ala^{1875} does not have phi-psi angles compatible with proline.

A key question regarding the spectrin-ankyrin interaction is how ankyrin maintains its interaction with spectrin during extension of spectrin under mechanical load. Spectrin repeats undergo reversible forced unfolding as spectrin tetramers are stretched in response to shear stresses impingent on the plasma membrane (5, 6). Despite this unfolding, the attachment of spectrin to membranes remains intact over a broad range of shear stresses (27, 28), suggesting that the ankyrin linkage to repeat 15 of β-spectrin is maintained even while spectrin repeats are unfolding in response to extension force. Our data, together with previous molecular dynamics simulations of forced unfolding of spectrin repeats, suggest a possible mechanism for how ankyrins maintain their spectrin association. Forced unfolding using atomic force microscopy shows that spectrin repeats unfold through a series of stable intermediates as the ends of spectrin repeats are pulled apart (29). Molecular dynamics simulations of these extensions suggest that a segment centered on the BC-loop is remarkably well preserved in these intermediates (29). The ability of ankyrin to bind to loop-15BC may thus allow ankyrin to maintain its interaction with spectrin even when repeat 15 exists in non-native conformations.

Acknowledgments—We thank Jan Hoffman for assistance with the yeast two-hybrid experiments and Brenda Pallares for administrative support.

REFERENCES

1. Mohandas, N., Chasis, J. A., and Shohet, S. B. (1983) *Semin. Hematol.* **20,** 225–242
2. Bennett, V., and Baines, A. J. (2001) *Physiol. Rev.* **81,** 1353–1392
3. Mohler, P. J., and Bennett, V. (2005) *Front. Biosci.* **10,** 2832–2840
4. Bennett, V., and Healy, J. (2008) *Trends Mol. Med.* **14,** 28–36
5. Rief, M., Pascual, J., Saraste, M., and Gaub, H. E. (1999) *J. Mol. Biol.* **286,** 553–561
6. Johnson, C. P., Tang, H. Y., Carag, C., Speicher, D. W., and Discher, D. E. (2007) *Science* **317,** 663–666
7. Kennedy, S. P., Warren, S. L., Forget, B. G., and Morrow, J. S. (1991) *J. Cell Biol.* **115,** 267–277
8. Dubreuil, R. R. (2006) *J. Membr. Biol.* **211,** 151–161
9. Minor, W., Cymborowski, M., Otwinowski, Z., and Chruszcz, M. (2006) *Acta Crystallogr. Sect. D Biol. Crystallogr.* **62,** 859–866
10. Schneider, T. R., and Sheldrick, G. M. (2002) *Acta Crystallogr. Sect. D Biol. Crystallogr* **58,** 1772–1779
11. Otwinowski, Z. (1991) in *Isomorphous Replacement and Anomalous Scattering* (Wolf, W., Evans, P. R., and Leslie, A. G. W., eds) pp. 80–86, Science & Engineering Research Council, Cambridge
12. Cowtan, K., and Main, P. (1998) *Acta Crystallogr. Sect. D Biol. Crystallogr* **54,** 487–493
13. Morris, R. J., Zwart, P. H., Cohen, S., Fernandez, F. J., Kakaris, M., Kirillova, O., Vonrhein, C., Perrakis, A., and Lamzin, V. S. (2004) *J. Synchrotron Radiat.* **11,** 56–59
14. Jones, T. A., Zou, J. Y., Cowan, S. W., and Kjeldgaard, M. (1991) *Acta Crystallogr. Sect. A* **47,** 110–119
15. Emsley, P., and Cowtan, K. (2004) *Acta Crystallogr. Sect. D Biol. Crystallogr.* **60,** 2126–2132
16. Murshudov, G. N., Vagin, A. A., and Dodson, E. J. (1997) *Acta Crystallogr. Sect. D Biol. Crystallogr.* **53,** 240–255
17. Davis, I. W., Leaver-Fay, A., Chen, V. B., Block, J. N., Kapral, G. J., Wang, X., Murray, L. W., Arendall, W. B., III, Snoeyink, J., Richardson, J. S., and Richardson, D. C. (2007) *Nucleic Acids Res.* **35,** W375–W383
18. Guex, N., and Peitsch, M. C. (1997) *Electrophoresis* **18,** 2714–2723
19. Beck, K., and Brodsky, B. (1998) *J. Struct. Biol.* **122,** 17–29
20. Hartwig, J. H. (1995) *Protein Profile* **2,** 703–800
21. Kusunoki, H., Minasov, G., Macdonald, R. I., and Mondragon, A. (2004) *J. Mol. Biol.* **344,** 495–511
22. Shotton, D. M., Burke, B. E., and Branton, D. (1979) *J. Mol. Biol.* **131,** 303–329
23. Bennett, V., Davis, J., and Fowler, W. E. (1982) *Nature* **299,** 126–131
24. Gallagher, P. G., and Forget, B. G. (1998) *Blood Cells Mol. Dis.* **24,** 539–543
25. Stabach, P. R., and Morrow, J. S. (2000) *J. Biol. Chem.* **275,** 21385–21395
26. Burridge, K., Kelly, T., and Mangeat, P. (1982) *J. Cell Biol.* **95,** 478–486
27. Discher, D. E., Mohandas, N., and Evans, E. A. (1994) *Science* **266,** 1032–1035
28. Mohandas, N., and Evans, E. (1994) *Annu. Rev. Biophys. Biomol. Struct.* **23,** 787–818
29. Altmann, S. M., Grunberg, R. G., Lenne, P. F., Ylanne, J., Raae, A., Herbert, K., Saraste, M., Nilges, M., and Horber, J. K. (2002) *Structure* (*Lond.*) **10,** 1085–1096